Preparation and Properties of Waterborne Interpenetrating Polymer Networks Composed of Polyurethaneurea and Graft Vinyl Ester Resin

Teng Su,[1,2] Chun Pu Hu[1,2]

[1]Key Laboratory for Ultrafine Materials, Ministry of Education, Shanghai 200237, People's Republic of China
[2]School of Materials Science and Engineering, East China University of Science and Technology, Shanghai 200237, People's Republic of China

ABSTRACT: Various waterborne interpenetrating polymer networks (IPNs) composed of polyurethaneurea (PUU) and graft vinyl ester resin were prepared from polyester polyol, dimethylolpropionic acid, isophorone diisocyanate, ethylenediamine and a well-defined graft vinyl ester resin containing butanol side chains (BO-g-VER). These anionic IPN aqueous dispersions were stable at the ambient temperature for >1 yr, and also had the excellent stability at low and high temperatures. The experimental results showed that the introduction of BO-g-VER network has not only greatly affected the particle morphology, stability and rheological behavior of these aqueous dispersions, but also rendered the films with the augmented surface hydrophobicity as well as the excellent water-resistance performance and mechanical properties. A synergistic effect was observed at a certain BO-g-VER composition (20 wt %) to give significant reinforcement to the PUU, resulting from the compatibility and/or the interpenetration between the PUU network and the BO-g-VER network. © 2009 Wiley Periodicals, Inc. J Appl Polym Sci 114: 1070–1079, 2009

Key words: compatibility; dispersions; graft vinyl ester resin; interpenetrating networks; waterborne polyurethaneurea

INTRODUCTION

Recently, for environmental requirements on minimizing the volatile organic compounds, waterborne polyurethane (PU) or polyurethaneurea (PUU),[1,2] and polyurethaneurea/acrylate polymer (PUA) aqueous dispersions[3,4] have gained rapid progress and found wide utilization in coatings, adhesives as well as surface finishes for textiles and leathers. However, the built-in hydrophilic moieties functioning as self-emulsifier in the macromolecular chain inevitably render waterborne PU, PUU, or PUA with undesirable water resistance and surface hydrophilicity in industrial applications. A number of approaches, such as crosslinking,[5] graft, and block copolymerization with various acrylate monomers[6,7] have been suggested and put into practice. In our laboratory, some silicon- or fluorine-containing hydrophobic units,[8–10] the well-defined hard segments[11] as well as the aromatic diamine extender[12] have also been introduced into these systems for enhancing the waterproof performance.

Interpenetrating polymer network (IPN) is defined as a unique class of polymer alloys consisting of two or more network polymers held together predominantly by permanent entanglement rather than by covalent bond grafting.[13] The IPNs have been studied extensively because most of them combine the characteristics of different polymers and exhibit better physical and mechanical properties than their individual networks due to a synergistic effect induced by the forced compatibility of the components and restricted phase separation. Recently, the waterborne PU IPNs have been also studied. Lee et al.[14] synthesized a series of PU/polystyrene (PS) latex IPNs by a two-stage emulsion polymerization of the hydrophilic vinyl terminated PU network and PS network. The tensile strength of the IPN films increased with increasing the amount of PS, and the content of water absorption decreased when the PS composition was >30 wt %. Kim and Shin[15] prepared the PU/poly(acrylic rubber) latex IPNs with enhanced degree of interpenetration observed by dynamic mechanical analysis, and found the increase in tensile strength and hydrophobicity of the IPN films. Chen and Chen[16] also reported the preparation of PU/polyacrylate (PA) latex IPNs with better water resistance and mechanical properties than the pure PU and the PU/PA blend.

In our laboratory, the vinyl ester resin (VER) has been synthesized by reacting epoxy resin with methacrylic acid, and the simultaneous interpenetrating networks (SINs) consisting of this kind of VER and PU have been further synthesized and studied for the reinforced reaction injection molding (RRIM) process.[17] The kinetics of the fast network formation for these SINs has been monitored during the RRIM process, and the relationship between their mechanical properties and the morphological development has been investigated.[18,19] Furthermore, for avoiding the formation of any chemical bonds between the two networks in SIN and enhancing the interpenetration between the two networks, a series of well-defined graft VERs consisting of urethane groups in the side chains were synthesized and characterized. The SINs prepared with PU and such graft VERs showed the real IPN structure and the reinforced mechanical properties.[20,21] In this article, the waterborne IPNs composed of the PUU and the well-defined graft VER containing butanol side chains were prepared and reported. The experimental data showed that the aqueous dispersions of these IPNs possessed even better stability and lower viscosity than the comparable waterborne PUU, and the IPN films exhibited the significantly enhanced waterproof performance and mechanical properties.

EXPERIMENTAL

Materials

Bisphenol A-type epoxy resin (E-51) was produced by Shanghai Synthetic Resin Plant (Shanghai, China), the epoxy value was tested as 0.513 mol epoxide/100 g resin. 2,4-Tolune diisocyanate (2,4-TDI) was provided by Shanghai Chemical Reagents Company (Shanghai, China) and was purified by fractional distillation under vacuum before use. 1-Butanol (BO) was analytic reagent provided by Shanghai Linfeng Chemical Reagents Company (Shanghai, China), dried with anhydrous K_2CO_3 and distilled before use. Methyl methacrylate (MMA) was produced by Shanghai Chemical Reagents Company (Shanghai, China), washed with 5 wt % NaOH and deionized water for several times, dehydrated with anhydrous $CaCl_2$ and CaH_2 for 2 days, respectively, and then distilled under vacuum before use. 2,2′-Azobisisobutyronitrile (AIBN) was filtered and recrystallized from hot 95 wt % ethanol, then dried under vacuum at room temperature. Difunctional poly(neopentylene adipate) polyol (P756, hydroxyl number = 56 mg KOH/g) was produced by Qingdao Yutian Chemical Company (Qingdao, China) and was dried under vacuum at 110°C for 2 h. Dimethylolpropionic acid (DMPA) was provided by Perstorp Company (Perstorp, Sweden) and was dried under vacuum at 60°C for 24 h. Isophorone

diisocyanate (IPDI) was supplied by Hüls Company (Frankfurt, Germany). Other materials were standard laboratory reagents and were used as received, except that N-methylpyrrolidone, triethylamine, and ethylenediamine (EDA) were treated with 0.4 nm molecular sieves for over 1 wk before use.

Synthesis of graft VER

First, 1 mol of BO was reacted with 1 mol of 2,4-TDI at 50°C to synthesize the NCO-terminated BO (named BO-NCO), until the value of NCO content measured according to ASTM D2572-80 was consistent with the theoretical value. Second, 2 mol of α-methacrylic acid was reacted with 1 mol of epoxy resin (E-51) using tetrabutyl ammonium bromide as catalyst to synthesize the methacrylate-terminated vinyl ester oligomer (VEO). Finally, the secondary hydroxyl groups existing in VEO were capped with BO-NCO, in the presence of dibutyltin dilaurate (DBTDL, 2.0×10^{-2} wt % of VEO) as catalyst at 50°C, to synthesize the graft VEO until the NCO content was lower than 0.02 wt %. The MMA, as comonomer, was then introduced into this graft VEO to prepare the graft VER (graft VEO/MMA = 64/36, wt/wt), designated as BO-g-VER. The synthetic schemes for the BO-NCO, VEO, graft VEO, and graft VER are shown in Figure 1. All the synthesis and characterization of these special chemical compounds synthesized here were described elsewhere in detail.[18–21]

Preparation of the PUU / graft VER IPN aqueous dispersions and their films

A stoichiometric amount of P756, DMPA, and IPDI ([NCO]/[OH] = 1.7, molar ratio) were charged into a 250-mL, four-necked flask equipped with a mechanical stirrer, a nitrogen inlet, a condenser, and a thermometer, and the mixture was reacted at 90°C for 4 h under a dry nitrogen atmosphere until the theoretical NCO value was reached. The obtained NCO-terminated prepolymer was neutralized by the addition of tertiary amine at 50°C for 40 min, and then BO-g-VER was introduced and mixed well with the system. The prepolymer/BO-g-VER mixture was then dispersed into deionized water under vigorous stirring at 40°C. Subsequently, EDA was added into the dispersion for the chain extension of prepolymer, followed by the addition of AIBN for the copolymerization of BO-g-VER at 70°C. PUU / BO-g-VER IPN aqueous dispersions were prepared with different weight ratios of the two components, namely, 80/20, 70/30, 60/40. For comparison, the pure PUU aqueous dispersion (WPUU) was also prepared according to the similar procedure without adding graft VER. The concentration of DMPA and hard segments in the PUU macromolecular chains were 6.7 and 31.3 wt %
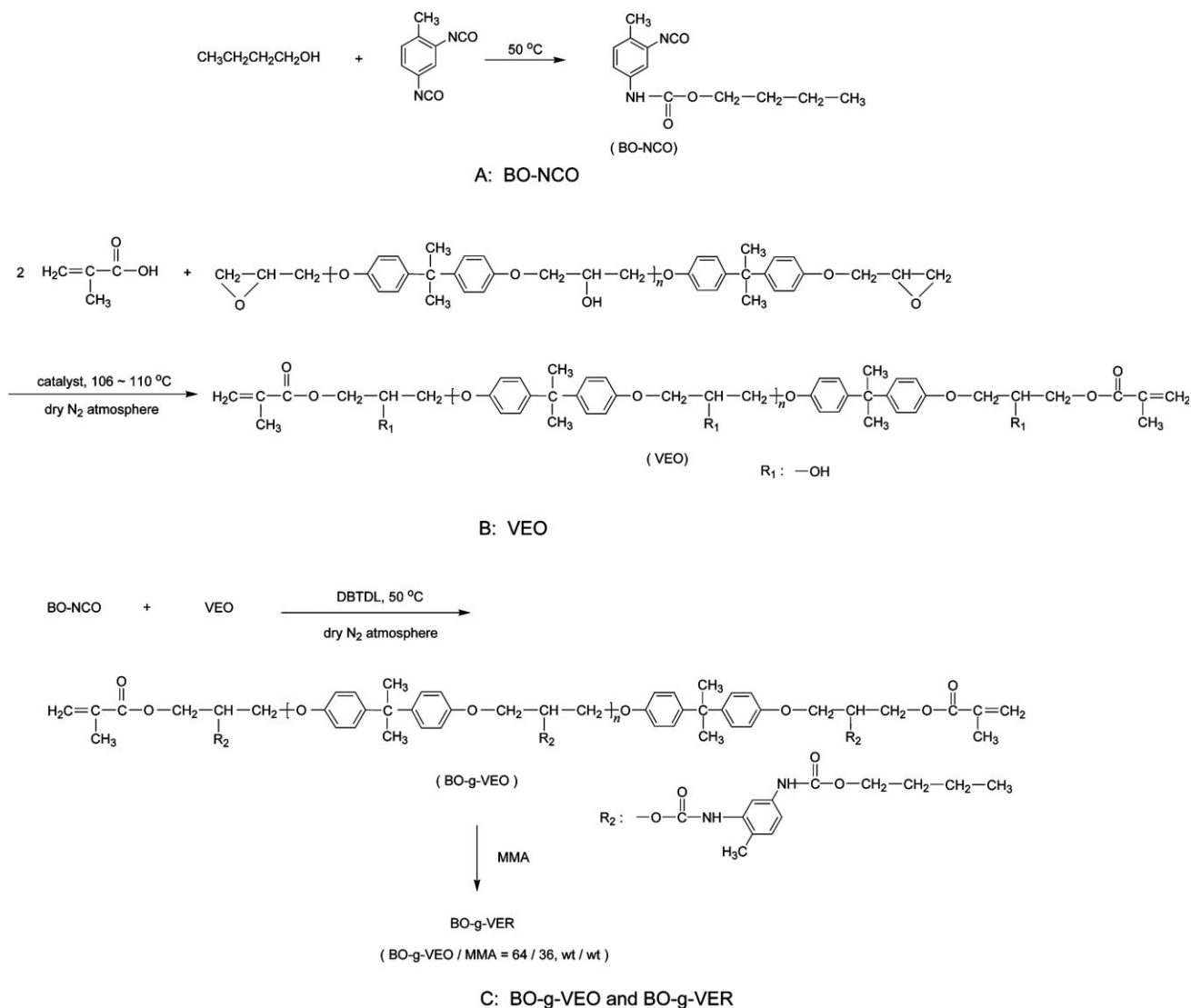
Figure 1 Synthetic schemes of BO-NCO (A), VEO (B), BO-g-VEO, and BO-g-VER (C).

(based on the total mass of PUU), respectively. All the aqueous dispersions had a solid concentration of ∼ 30 wt %.

The PUU/BO-g-VER IPN and the PUU films were prepared by casting the aqueous dispersions into Teflon molds at 25°C. Then, they were dried at 25°C for 7 days and under vacuum at 60°C for 24 h until a constant weight was obtained.

Characterization

The particle size and distribution of the aqueous dispersions were measured by dynamic laser light scattering on a Malvern Zetasizer 3000, where a He-Ne type laser (wavelength 633 nm, scattering angle 90°) was used. Approximately 0.15 mL of the dispersion sample was diluted with deionized water to 0.5 wt % and directly placed in the capillary cell, which

was kept at 25°C. The rheological properties of the aqueous dispersions were measured with a Haake RheoStress 600 rheometer at 25°C. The zeta potentials of the aqueous dispersions were tested at different pH values with a Brookhaven Zeta Plus at 25°C. The pH values were determined with a Mettler Toledo DELTA 320 analyzer. The high-temperature stability of the aqueous dispersions was determined by the observation of whether the aqueous dispersions were deposited or not after being placed in an oven at 60°C for 40 h. For freeze-thaw stability measurements, the PUU aqueous dispersions were subjected to a number of testing cycles, in which the samples were frozen at −30°C for 18 h and then allowed to thaw at room temperature for 6 h. At least five cycles were performed for each sample to observe whether any precipitation could be detected. The stability of the aqueous dispersion was expressed by the recycle times of the freeze-thaw test.

Sample	BO-g-VER content (wt %)	Particle size (nm)	Polydispersity	Thermal stability (h)	Freeze-thaw stability (cycle)	n[b]	K[c]
WPUU	0	51	0.21	28	3	0.89	0.212
PUU/BO-g-VER (80/20)	20	78	0.15	>40	>10	0.92	0.041
PUU/BO-g-VER (60/40)	40	84	0.09	>40	>10	0.99	0.010

[a] None of the aqueous dispersions, except for WPUU, deposited after storage for 1 yr at the ambient temperature.
[b] Flow behavior index.
[c] Consistency coefficient.

The critical coagulation concentration (ccc) of the aqueous dispersions was tested at 25°C using a phenomenological approach. Two milliliters of the dispersion sample was added into an agitated test tube containing the same volume of NaCl aqueous solution. The concentration of the NaCl solution was adjusted to cover a concentration range increasing from 0.1 to 2.0 mol/L with a step of 0.01 mol/L. Beyond the ccc, coagulation was observed almost instantaneously as expected. The limiting concentration before the rapid coagulation of the dispersion is used as an indicative value for the ccc.

The density of the film prepared from the dispersion sample (d_p) was determined according to the following procedure. Deionized water was charged into a pycnometer and weighed as W_1 after being kept at 25°C for 30 min, followed by the addition of a piece of preweighed (W_2) dry film sample. Subsequently, the above-mentioned matter was kept at 25°C for further 15 min, and the total mass was determined to be W_3. Therefore, the value of d_p is given by:

$$d_p = \frac{W_2}{W_1 + W_2 - W_3} \times d_{water} \qquad (1)$$

where d_{water} is the density of deionized water at 25°C.

The transmission Fourier transform infrared (FTIR) spectra of the PUU / BO-g-VER IPN films were recorded with a Nicolet Magana IR 5700 FTIR spectrometer at 25°C. The mechanical properties of all the specimens were conducted on a Shimadzu AG-2000A testing machine under a 50 mm/min crosshead rate, and the specimens were made in accordance with GB1040-79. The Shore A hardness of the specimens was measured according to ASTM D 2240-85.

The amount of the water absorption of the films (25 mm × 25 mm × 1 mm) was tested in water for 24 h at 25°C and was calculated as follows:

$$Water\ absorption(\%) = (W_2 - W_1)/W_1 \times 100\% \qquad (2)$$

where W_1 and W_2 are the weights of the film before an after soaking, respectively.

The contact angle of water or ethylene glycol on the air-side surface of the film sample was measured with the sessile drop method at 25°C by using a JC2000A series instrument, and an average of five replicas was recorded.

RESULTS AND DISCUSSION

IPN aqueous dispersions

The IPN aqueous dispersions were prepared by a sequential two-stage polymerization process. Initially, the PU prepolymer was chain extended with EDA, and then the PUU network was formed with the both aids of the EDA generating chemical-crosslinking sites and the intermacromolecular hydrogen bonding acting as physical-crosslinking sites (It will be discussed later). The BO-g-VER network was then produced, in the presence of the PUU network, by the free-radical copolymerization of MMA with the graft VEO in which both ends of the macromolecular chains were capped with double bonds. This kind of free radical copolymerization is performed easily, because the butanol side chains would not compromise the activity of the terminal double bonds in the graft oligomer.[20,21] In this case, each particle in the aqueous dispersion should be regarded as the PUU / BO-g-VER IPN.

Table I lists some physical properties of the PUU/BO-g-VER IPN aqueous dispersions with different composition. With increasing BO-g-VER network composition, the particle size distribution decreased and the particle size increased, but it was still <100 nm. In WPUU system, owing to the DMPA units containing carboxylate groups, the PUU particles exhibit the hydrophilic nature that would facilitate the formation of hydrogen bonding between the PUU and the water molecules. This gives rise to forming somewhat thick hydration layer onto the particle surface and irregular particle shape. Therefore, the high polydispersity index of the PUU aqueous dispersion is usually observed. With introducing BO-g-VER accompanied by the formation of interpenetrating network structure, the particles of the IPN dispersion became rigid and approached the regular

spherical shape. As a result, the markedly low polydispersity index of IPN (60/40) should be expected.

The particle size of a PUU aqueous dispersion is primarily dependent on the number of the hydrophilic units, as well as the chemical composition and the electric charge distribution of the particle surface. To investigate the particle surface composition, the variations of the zeta potential as a function of pH value for all the IPN aqueous dispersions were tested, as depicted in Figure 2. Figure 2 shows that the isoelectric points of IPN (80/20) and IPN (60/40) were close to that of WPUU system (around pH = 3.7). With the increase of BO-g-VER, the values of zeta potential for the IPN systems shifted slightly toward the negative direction, however, generally adjacent to those of WPUU within the whole pH range. These results indicated that the graft VER network in the IPN were mostly encapsulated by the PUU network, and the particle surface of the aqueous dispersion generally exhibited the electrical nature similar to those of pure PUU particles. However, the surface composition of the particles has been somewhat changed with the introduction of interpenetrating structure. With increasing BO-g-VER composition, the copolymerization of MMA, and graft VEO within the hydrophilic PUU particles would give rise to an increase in particle size in the IPN aqueous dispersion. At the same time, as more hydrophobic BO-g-VER network were resident inside the particle, more hydrophilic carboxylate groups would be driven to orient at the polymer-water interface, resulting in an increase in the number of anions distributed on the surface of the particle. Therefore, a slight increase of the absolute values of zeta potential should be expected with the increase of BO-g-VER composition.

Table I also indicates that the IPN aqueous dispersions exhibited better high temperature and freeze-thaw stability than the pure PUU specimen. Furthermore, these IPN aqueous dispersions still remained stable after the storage over 1 yr at the ambient temperature, whereas considerable precipitation had been observed in the comparable WPUU system. These features are very important for an aqueous dispersion further applied in industries.

According to the Derjaguin-Landau-Verwey-Overbeek theory, in the assumption of negligible steric or entropic repulsion, the overall stability of an electrostatically stabilized colloid is contributed from two factors: the repulsive electrical double layer (EDL) term and the attractive van der Waals term.[22,23] In terms of the interaction of two approaching particles, the free energy contribution of the EDL repulsion is given by,

$$V_R = \frac{32\pi\varepsilon\varepsilon_0 (k_B T)^2 R}{z^2 e^2} \tanh^2\left(\frac{ze\psi_s}{4k_B T}\right)\exp(-\kappa H) \quad (3)$$
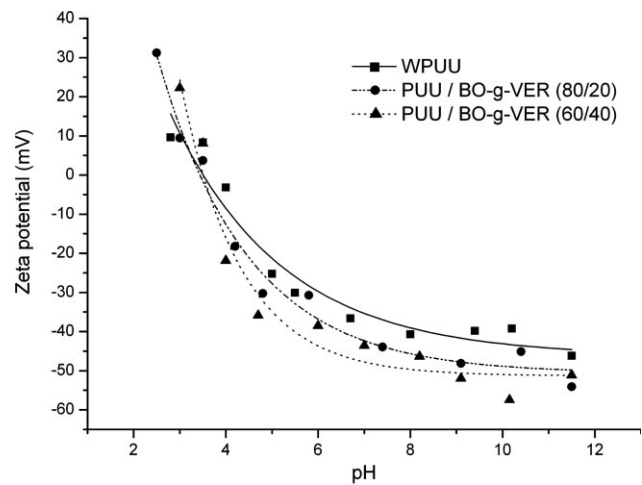

Figure 2 Zeta potential versus the pH for the different aqueous dispersions.

and the van der Waals attraction is expressed as,

$$V_A =$$
$$-\frac{A}{6}\left(\frac{2R^2}{H(4R+H)} + \frac{2R^2}{(2R+H)^2} + \ln\left(\frac{H(4R+H)}{(2R+H)^2}\right)\right) \quad (4)$$

where R is the particle radius, H is the distance between the particle surface, A is the Hamaker constant, ψ_s is the surface (Stern) potential, z is the electrolyte valence, T is the absolute temperature, k_B is Boltzmann constant, e is the elementary charge, ε is the relative dielectric constant of the continuous medium, ε_0 is the permittivity of vacuum, and κ is the reciprocal of the Debye length (also defined as the thickness of the diffuse part of the EDL).

For $H/2R \ll 1$, the attractive energy in eq. (4) becomes,

$$V_A = -\frac{AR}{12H} \quad (5)$$

The total pair potential V_T is the sum of the two contributions,

$$V_T = V_A + V_R \quad (6)$$

The increase of the concentration of electrolyte in the system will compress the EDL and reduce the electrostatic repulsion between the particles, rendering the system with an unstable nature. The electrolyte concentration at which the energy barrier vanishes is known as the ccc, which is associated with ψ_s as follows[24]:

$$ccc = 3.853 \times 10^{-39}\gamma^4/A^2 z^6 \quad (7)$$

$$\gamma = [\exp(ze\psi_s/2k_B T) - 1]/[\exp(ze\psi_s/2k_B T) + 1] \quad (8)$$

It is noticed that the surface potential ψ_s is difficult to be measured directly, but the zeta potential,

Sample	d_p (g·cm^{-3})	ζ Potential (mV)	ccc (mol·L^{-1})	V_A (J)	V_R (J)	V_T (J)
WPUU	1.08	−41.7	0.80	-1.12×10^{-21}	7.76×10^{-20}	7.65×10^{-20}
PUU/BO-g-VER (80/20)	1.08	−47.3	0.75	-1.45×10^{-21}	9.66×10^{-20}	9.52×10^{-20}
PUU/BO-g-VER (60/40)	1.07	−50.6	0.86	-1.58×10^{-21}	1.12×10^{-19}	1.10×10^{-19}

[a] The data were obtained at pH = 9.10 under 25°C.

which can be tested experimentally from electrokinetic measurements, is generally accepted as a fair approximation for the value of ψ_s.[25]

To give an quantitative comparison of the colloidal stability for the IPN aqueous dispersions with different composition, the values of V_A, V_R, and V_T were calculated in combination of eqs. (3)–(8), and listed in Table II. It was found that the total potential of the IPN system was primarily determined by the electrostatic repulsion term, and increased with the increase of BO-g-VER composition. These calculations indicated that the introduction of graft VER forming interpenetration network with the PUU network was favorable for enhancing the stability of the aqueous dispersion system, as consistent with the experimental results.

Figure 3 shows the viscosity as a function of shear rate ($\dot\gamma$) at 25°C for different IPNs. The $\dot\gamma$-dependence of the shear stress (τ) was also recorded for these systems. This dependence could be well-described by a power law expressed as the following equation[26] with the experimental data, as shown in Figure 4.

$$\lg \tau = \lg K + n \lg \dot\gamma \tag{9}$$

where n is the flow behavior index, and K is the consistency coefficient which is proportional to the fluid's viscosity. The values of n and K were com-puted using a linear regression method and listed in Table I.

Figures 3 and 4 indicate that the WPUU system exhibited the highest viscosity over all the specimens tested, but its viscosity decreased evidently with the increase of shear rate, showing a typical pseudoplastic fluid. The IPN systems, however, exhibited the notably different rheological behavior close to the Newtonian flow, and PUU / BO-g-VER (60/40) IPN could be considered as a typical Newtonian fluid (n = 0.99) with the lowest viscosity independent of the shear stress.

The WPUU specimen showed the shear-thinning behavior, due to the hydrophilic DMPA groups on particle surface inducing the strong electrostatic interactions between the negatively-charged particles and the counterions in the EDL as well as the hydrogen bonding between the PUU and the water molecules, which would be readily broken down with increasing external shear force. For the IPN systems, the significant decrease of the viscosity with increasing BO-g-VER composition could be ascribed to the interaction between the BO-g-VER network and the DMPA units, which decreased the ability of carboxylate groups to form hydration layer onto the particle surface.

Wang et al.[20] reported that the side chains containing urethane groups in the BO-g-VER network

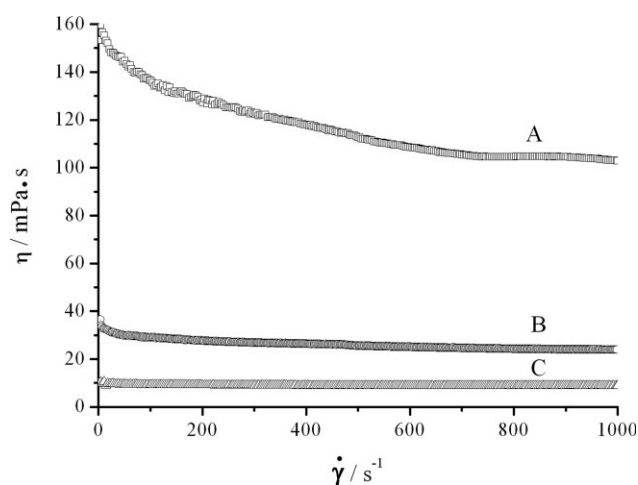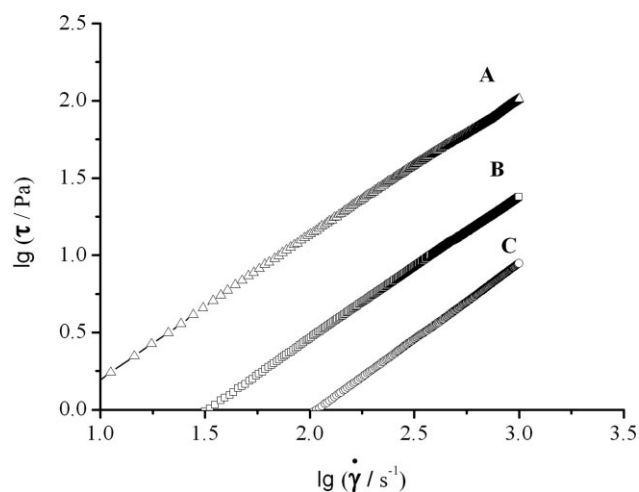Figure 3 Viscosity versus shear rate for the different aqueous dispersions at 25°C (A) WPUU; (B) PUU/BO-g-VER (80/20); (C) PUU/BO-g-VER (60/40).

Figure 4 lg τ versus lg $\dot\gamma$ for the different aqueous dispersions at 25°C (A) WPUU; (B) PUU/BO-g-VER (80/20); (C) PUU/BO-g-VER (60/40).

TABLE III
Some Physical Properties of the PUU/BO-g-VER IPN Films

Sample	Water absorption, 24 h (wt %)	Contact angles (°) Water	Ethylene glycol	γ_s (mN/m)	γ_s^p (mN/m)	γ_s^d (mN/m)
WPUU	28.9	78	62	31.6	21.0	10.6
PUU/BO-g-VER (80/20)	15.1	84	66	28.1	17.1	11.0
PUU/BO-g-VER (70/30)	12.3	86	67	27.1	15.7	11.4
PUU/BO-g-VER (60/40)	9.5	88	68	26.2	14.3	11.9

were miscible with the hard segments in PU. In addition, the ester carbonyls in the MMA units were also miscible with the polyester soft segments in PUU and could form hydrogen bonding with the NH groups in urethane or urea linkages in PUU hard segments.[27] In this case, the BO-g-VER network in IPN should have compatibility with the PUU network (this behavior will be discussed in detail in the next section). Because the hydrophilic carboxylate groups were located in the hard segments in PUU network, when the BO-g-VER network was introduced to form IPN, the mobility of these hydrophilic groups could be constrained due to the compatibility between the BO-g-VER network and the PUU hard segments, so that they were not easy to form hydrogen bonds with water molecules because of steric hindrance. Consequently, the particles became weak in hydration, and then the interactions among particles might also be weakened.

Generally, for an aqueous dispersion, the relationship between the viscosity and the volume fraction is described by the Mooney equation[28,29]:

$$\eta_r = \exp\left[\frac{2.5\Phi}{1 - (\Phi/\Phi_m)}\right] \qquad (10)$$

where η_r is the relative viscosity of the aqueous dispersion defined as a ratio of the dispersion viscosity to the continuous phase viscosity, Φ is the volume fraction of the dispersed phase, and Φ_m is the maximum or critical volume fraction, which assumes a value of 0.74 for the most densely packed spheres (hexagonal close packing) and a value of 0.52 for loosely packed monodisperse spheres (cubical close packing) without interaction. The decrease in hydration would give rise to decreasing the volume fraction of the dispersed phase, hence decreasing the viscosity of the system. Therefore, the increase of BO-g-VER composition should further reduce the viscosity of the IPN aqueous dispersion.

Meanwhile, the incorporation of BO-g-VER network rendered the polymer particles with increasing rigidity. This would make the IPN particles become difficult to deform under shear force. Therefore, with the increase in BO-g-VER composition, the volume fraction of the dispersed phase became immune to the external shear stress, resulting in a constant

viscosity for the system according to the Mooney theory. As a result, the PUU/BO-g-VER (60/40) IPN showed a typical Newtonian behavior.

IPN films

Table III shows the amounts of water absorption and some surface properties of the films prepared with the IPN aqueous dispersions. The surface energy for a polymer film is difficult to measure directly, but it can be calculated indirectly through the measurement of the equilibrium contact angles of some standard liquids, that is, water and ethylene glycol, on the air side of its surface[30]:

$$(1 + \cos\theta_1)\gamma_1 = 4\left(\frac{\gamma_1{}^d\gamma_s^d}{\gamma_1^d + \gamma_s^d} + \frac{\gamma_1^p\gamma_s^p}{\gamma_1^p + \gamma_s^p}\right) \qquad (11)$$

$$(1 + \cos\theta_2)\gamma_2 = 4\left(\frac{\gamma_2{}^d\gamma_s^d}{\gamma_2^d + \gamma_s^d} + \frac{\gamma_2^p\gamma_s^p}{\gamma_2^p + \gamma_s^p}\right) \qquad (12)$$

$$\gamma_s = \gamma_s^d + \gamma_s^p \qquad (13)$$

where θ_1 and θ_2 are the contact angles of water and ethylene glycol on the surface of the polymer film, respectively; γ_s, γ_s^d, and γ_s^p are the surface energy, dispersion component, and polar component for the polymer films, respectively; γ_1, γ_1^d, and γ_1^p are the surface tension, dispersion component, and polar component for water ($\gamma_1^d = 21.8$ mN/m, $\gamma_1^p = 51.0$ mN/m), respectively; γ_2, γ_2^d, and γ_2^p are the surface tension, dispersion component, and polar component for ethylene glycol ($\gamma_2^d = 29.3$ mN/m, $\gamma_2^p = 19.0$ mN/m), respectively.[30]

With increasing BO-g-VER composition in IPN, the water absorption amount of the films decreased remarkably from 28.9 to 9.5 wt %, the contact angle of water on the film surface increased from 78° to 88°, and the calculated surface energy decreased gradually in comparison with the control specimen. These results should arise from the good hydrophobic nature of epoxy backbone existing in the BO-g-VER network as well as the good compatibility and/or interpenetration between PUU and BO-g-VER network. In addition, for the IPN systems, the decrease
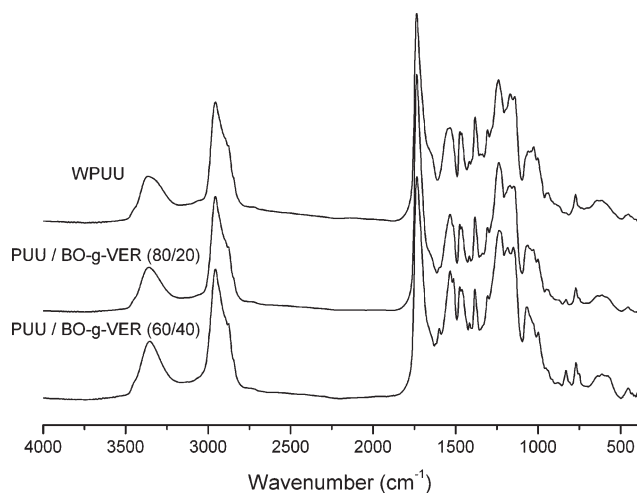
Figure 5 FTIR absorption curves for the different PUU/BO-g-VER IPNs.

of γ_s mainly came from the decrease of γ_s^p. This might be explained by the enrichment of nonpolar butanol side chains on the film surface during the film-forming procedure. Table III also listed the physical properties of PUU/BO-g-VER (70/30) IPN. All the experimental data confirmed that the physical properties of IPNs were well related with the PUU/BO-g-VER composition, which was in accordance with the previous discussion.

Generally, the strong hydrogen bonding of the urethane and urea linkages for a multiblock PUU is easily formed. The ordered structure of hard segments in PUU should be related to the interactions of hydrogen bonding in the system and can be measured using FTIR spectrometer. Figure 5 shows the FTIR spectra of the PUU/BO-g-VER IPNs with different composition. In the infrared spectra of these specimens, the region at 1750–1600 cm^{-1} corresponding to the carbonyl stretching vibrations has been widely used to characterize the hydrogen bonding of PUUs. In this study, the hydrogen bonding between the urea linkages was chosen for investigation, as the absorption peaks for urethane groups would be affected by the carbonyl absorption peaks of the polyester segments in the PUU and the MMA units in the BO-g-VER network.[3,9,10] However, the carbonyl absorption peak of DMPA units existing in the PUU network is located at 1550 cm^{-1}, which would not influence the investigation of hydrogen bonding for urea groups.[3] Figure 6 shows the FTIR spectra of different IPNs in the carbonyl region at 25°C. In these spectra, multiple bands can be found. The iteration procedure of damping least squares, based on a combination of Lorentzian and Gaussian curve shapes, was used to separate the absorption peaks in the carbonyl region corresponding to different kinds of hydrogen bonding[3,31,32] (Table IV), and the curve-fitting results are listed in Table V. The
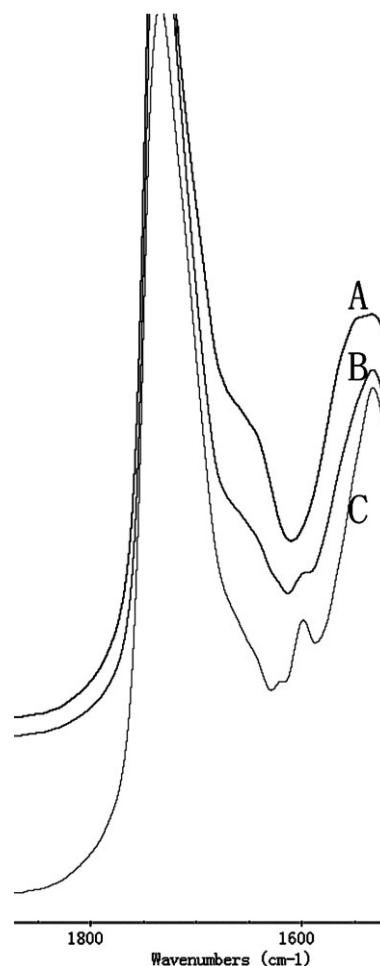

Figure 6 FTIR absorption spectra in the carbonyl region for the different PUU/BO-g-VER IPNs (A) WPUU; (B) PUU/BO-g-VER (80/20); (C) PUU/BO-g-VER (60/40).

degree of hydrogen bonding for urea groups ($X_{b,UA}$), and the percentages of ordered and disordered urea hydrogen bonds ($X_{o,UA}$ and $X_{d,UA}$) in Table V are defined as follows:

$$X_{b,UA} = \frac{\sum \text{Area(bonded)}}{\text{Area}(1690 \text{ cm}^{-1}) + \sum \text{Area(bonded)}} \quad (14)$$

TABLE IV
Assignment of the Absorption Bands in the Carbonyl Region of the FTIR Spectra for PUU/BO-g-VER IPNs

Wave number (cm^{-1})	Assignment
1747 – 1728	Free carbonyl stretching of urethane linkages, polyester, and methyl acrylate
1717 –1727	Disordered hydrogen-bonded carbonyl of urethane linkages, polyester and methyl acrylate
1708–1700	Ordered hydrogen-bonded urethane carbonyl
1690–1680	Free urea carbonyl
1678–1650	Disordered hydrogen-bonded urea carbonyl
1649–1640	Ordered II hydrogen-bonded urea carbonyl
1640–1632	Ordered I hydrogen-bonded urea carbonyl

TABLE V
Least-Square-Curve-Fitting FTIR Spectra in the Urea Carbonyl Region for the Different PUU/BO-g-VER IPNs

Sample	Peak area (%)					$X_{o,UA}$ (%)	$X_{d,UA}$ (%)	$X_{b,UA}$ (%)
	1690 (cm^{-1})	1675 (cm^{-1})	1660 (cm^{-1})	1642 (cm^{-1})	1632 (cm^{-1})			
WPUU	33.6	26.2	23.0	15.9	1.3	17.2	49.2	66.4
PUU/BO-g-VER (80/20)	48.7	3.2	39.6	4.9	3.6	8.5	42.8	51.3
PUU/BO-g-VER (60/40)	56.4	7.7	31.2	3.5	1.2	4.7	38.9	43.6

$$X_{o,UA} = \frac{\sum \text{Area}(1649 - 1632 \text{ cm}^{-1})}{\text{Area}(1690 \text{ cm}^{-1}) + \sum \text{Area(bonded)}} \quad (15)$$

$$X_{d,UA} = \frac{\sum \text{Area}(1678 - 1650 \text{ cm}^{-1})}{\text{Area}(1690 \text{ cm}^{-1}) + \sum \text{Area(bonded)}} \quad (16)$$

Table V shows that WPUU exhibited the high total hydrogen bonding degree of urea groups with the value of $X_{o,UA}$ as high as 17.2 %, indicating the existence of a considerable number of monodentate urea carbonyls and those forming the disordered hydrogen bonds with the NH groups in the urethane linkages. With the increase of BO-g-VER composition, the values of $X_{b,UA}$ and $X_{o,UA}$ decreased monotonically. A slight decrease of $X_{b,UA}$, but a markedly decrease of $X_{o,UA}$ was observed in PUU / BO-g-VER (80/20) IPN. This was because the BO-g-VER containing both the urethane linkages and the ester carbonyls were compatible with the hard segments in PUU, resulting in destroying the originally ordered structure in the PUU hard microdomain. With further increasing BO-g-VER composition, the suppression of the ordered hydrogen-bonding formation for the urea linkages became more pronounced in the PUU/BO-g-VER (60/40) IPN. In this case, this IPN aqueous dispersion should show low viscosity, as shown in Figure 4 and discussed before.

The mechanical properties of these IPN specimens were measured, as listed in Table VI. The PUU/BO-g-VER (80/20) IPN showed the maximum tensile strength as well as the elongation at break. When the BO-g-VER composition further increased to 40 wt %, the tensile strength and the elongation at break decreased, but the hardness of the IPN film was still high. These experimental results could be

attributed to the synergistic effect produced by the interpenetration and physical entanglements between two networks in IPN.

CONCLUSIONS

The well-defined graft VER (BO-g-VER) containing epoxy resin backbones and butanol side chains was synthesized via molecular design technique. A series of waterborne IPN aqueous dispersions and their films composed of BO-g-VER and anionic PUU with different compositions were prepared and characterized. With the increase in BO-g-VER composition, the IPN aqueous dispersions showed an evident increase in colloidal stability and decrease in viscosity, with a rheological transition from pseudoplastic to Newtonian flow. The IPN films displayed an enhancement in surface hydrophobicity as well as reduction in water absorption in comparison with the pure PUU film. A maximum synergy effect was observed at 20 wt % BO-g-VER content in terms of tensile strength and elongation at break of the PUU/BO-g-VER IPNs. The variation in physical properties of these IPN aqueous dispersions and their films was closely related with the PUU/BO-g-VER composition, which was ascribed to the interaction between the BO-g-VER network and the PUU network.

TABLE VI
Mechanical Properties of the Different PUU/BO-g-VER IPN Films

Sample	Hardness (shore A)	Tensile strength (MPa)	Elongation at break (%)
WPUU	83	22.7	425
PUU/BO-g-VER (80/20)	91	32.0	491
PUU/BO-g-VER (70/30)	93	27.6	266
PUU/BO-g-VER (60/40)	93	19.2	83

References

1. Cheong, I. W.; Kong, H. C.; An, J. H.; Kim, J. H. J Polym Sci Part A: Polym Chem 2004, 42, 4353.
2. Nanda, A. K.; Wicks, D. A.; Madbouly, S. A.; Otaigbe, J. U. Macromolecules 2006, 39, 7037.
3. Hu, Y. S.; Tao, Y.; Hu, C. P. Biomacromolecules 2001, 2, 80.
4. Pardini, O. R.; Amalvy, J. I. J Appl Polym Sci 2008, 107, 1207.
5. Sundar, S.; Aruna, P.; Venkateshwarlu, U.; Radhakrishnan, G. Colloid Polym Sci 2004, 283, 209.
6. Huybrechts, J.; Bruylants, P.; Vaes, A.; De Marre, A. Prog Org Coat 2000, 38, 67.
7. Kim, B. K.; Lee, J. S.; Lee, M. C.; Yoon, K. S. J Appl Polym Sci 2003, 88, 1971.
8. Li, H.; Zhang, Z. B.; Hu, C. P.; Wu, S. S.; Ying, S. K. Eur Polym J 2004, 40, 2195.
9. Su, T.; Wang, G. Y.; Xu, X. D.; Hu, C. P. J Polym Sci Part A: Polym Chem 2006, 44, 3365.
10. Su, T.; Wang, G. Y.; Hu, C. P. J Polym Sci Part A: Polym Chem 2007, 45, 5005.

11. Yang, D. Y.; Hu, C. P.; Ying, S. K. J Polym Sci Part A: Polym Chem 2005, 43, 2606.
12. Jiang, L.; Chen, Y. L.; Hu, C. P. J Coat Technol Res 2007, 4, 59.
13. Sperling, L. H. Interpenetrating Polymer Networks and Related Materials; Plenum: New York, 1981.
14. Lee, J. S.; Shin, J. H.; Kim, B. K.; Kang, Y. S. Colloid Polym Sci 2001, 279, 959.
15. Kim, B. K.; Shin, J. H. Colloid Polym Sci 2002, 280, 716.
16. Chen, S.; Chen, L. Colloid Polym Sci 2003, 282, 14.
17. Chen, N. P.; Chen, Y. L.; Wang, D. N.; Hu, C. P.; Ying, S. K. J Appl Polym Sci 1992, 46, 2075.
18. Fan, L. H.; Hu, C. P.; Ying, S. K. Polymer 1996, 37, 975.
19. Fan, L. H.; Hu, C. P.; Pan, Z. Q.; Zhang, Z. P.; Ying, S. K. Polymer 1997, 38, 3609.
20. Wang, G. Y.; Zhu, M. Q.; Hu, C. P. J Polym Sci Part A: Polym Chem 2000, 38, 136.
21. Wang, G. Y.; Wang, Y. L.; Hu, C. P. Eur Polym J 2000, 36, 735.
22. Shaw, D. J. Introduction to Colloid and Surface Chemistry, 4th ed.; Butterworths: London, 1992.
23. Fitch, R. M. Polymer Colloids: A Comprehensive Introduction; Academic Press: London, 1997;
24. Lovell, P. A.; El-Aasser, M. S. Emulsion Polymerization and Emulsion Polymers; John Wiley and Sons: New York, 1997.
25. Hidalgo-Alvarez, R.; Martin, A.; Fernandez, A.; Bastos, D.; Martinez, F.; De Las Nieves, F. J. Adv Colloid Interface Sci 1996, 67, 1.
26. Han, C. D. Rheology in Polymer Processing; Academic Press: New York, 1976.
27. Painter, P. C.; Veytsman, B.; Coleman, M. M. J Polym Sci Part A: Polym Chem 1994, 32, 1189.
28. Mooney, M. J Colloid Sci 1951, 6, 162.
29. Kulicke, W.-M.; Arendt, O.; Berger, M. Colloid Polym Sci 1998, 276, 1024.
30. Wu, S. H. Polymer Interface and Adhesion; Marcel Dekker: New York, 1982.
31. Luo, N.; Wang, D. N.; Ying, S. K. Polymer 1996, 37, 3045.
32. Wen, T. C.; Wu, M. S. Macromolecules 1999, 32, 2712.